Mechanism of Meniscus Oscillations and Stripe Pattern Formation in Langmuir−Blodgett Films

V. I. Kovalchuk,[†] M. P. Bondarenko,[†] E. K. Zholkovskiy,[†] and D. Vollhardt*[,‡]

Max-Planck-Institute of Colloids and Interfaces, 14424 Potsdam/Golm, Germany, and Institute of Biocolloid Chemistry, Kiev, Ukraine

Received: April 3, 2002; In Final Form: September 19, 2002

The mechanism of the meniscus oscillations and the stripes formation within the deposited fatty acid monolayer is theoretically analyzed on the basis of a supposition of concentration polarization within the solution during the deposition process. The concentration polarization can lead to decrease of adhesion work, dynamic contact angle, and maximum deposition speed under dynamic conditions resulting in meniscus instability. The adhesion work is evaluated from the disjoining pressure isotherm at a given subphase composition taking into account the charge regulation for a fatty acid monolayer. The relation of the proposed mechanism to the known experimental facts and observations is discussed.

Introduction

Langmuir−Blodgett films are important objects for many technical applications.[1] Their quality depends not only on the chemical nature of the constituents but also on the conditions of the film formation. In particular, instability arising during the monolayer transfer can influence the structure and the properties of the deposited monolayer. The study of this instability can provide us new information about the processes happening at the monolayer deposition and help us to understand the influence of the deposition conditions on the properties of the obtained LB-films.

Meniscus instability occurs when a monolayer of arachidic acid formed at the water surface is transferred to a solid surface at pH in the aqueous subsolution of ∼5.7 in the presence of cadmium salt.[2] It was observed that the meniscus is not stationary but can oscillate during the monolayer transfer (a "slip-stick" behavior): the meniscus height increases gradually with the substrate upstroke until a certain position and, then, decreases rapidly. The contact angle decreases with increase of the meniscus height. The meniscus becomes unstable when the contact angle tends to zero. As a consequence, the contact line recedes suddenly and the contact angle increases backward. The observed meniscus oscillations are accompanied by variations of the composition of the deposited film, which appeared to consist of alternating stripes of either arachidic acid or cadmium arachidate. Thus, the stationary contact angle is not observed at the experimental conditions of ref 2, and this effect has a relation to the compositional changes. The similar alternating "bands" within the arachidic acid/cadmium arachidate LB films at intermediate pH values (between 5.2 and 5.8), running perpendicular to the dipping direction, were reported also in ref 3.

Analogous stripe patterns of phospolipid (DPPC) monolayers on the SiO_2 surface, but independent of the pH, were found in refs 4−7. However, the stripes within the LB films of DPPC are formed when the surface pressure is kept close to the point of phase transition from the liquid-expanded to liquid-condensed phase. The deposition in more or less condensed two-dimensional phases induced due to, so-called, substrate-mediated condensation explains this stripes formation, as supposed. In the case of fatty acid monolayers, a phase transition (as the floating monolayer is already in a condensed phase) does obviously not take place but rather a transition from arachidic acid to cadmium arachidate in the narrow pH range close to pH = 5.7. Thus, the stripe structures found by the transfer of DPPC monolayers are obviously caused by another mechanism.

The problem of meniscus stability during the process of a charged monolayer transfer to a solid surface comprises a number of aspects. They are the overlapping of the electrical double layers in the meniscus region, binding of the counterions, changes in the monolayer charge and composition, and changes in the surface potential due to interaction with the substrate. Also, at dynamic conditions, one can expect complicated hydrodynamic processes produced by the moving surfaces, deviations of the distributions of ions and potential in the subphase from equilibrium, and variations of the meniscus shape and contact angle as a consequence of the violation of the balance of molecular, electrical, viscous, and gravity forces.

Some of these aspects were discussed in our previous paper.[8] It was shown that, in the meniscus region, under the experimental conditions given in ref 2, the changes in the monolayer composition and in the surface potential are not significant when equilibrium holds. However, according to ref 8, the charge of the monolayer approaches to zero in vicinity of the three-phase contact line due to the binding of the counterions Cd^{2+} and H^+ from the subsolution. On the other hand, at dynamic conditions, the variation of the monolayer composition can be larger and can influence the contact angle, the meniscus shape, and stability.

The objective of the present work is to propose a mechanism for the meniscus oscillations and the stripes formation within the deposited fatty acid monolayer on the basis of a variation of the local subphase composition during the deposition process. The main idea is that the variation of the local subphase composition under dynamic conditions can lead to decrease of adhesion work, contact angle, and maximum deposition speed.

* Corresponding author.
[†] Institute of Biocolloid Chemistry.
[‡] Max-Planck-Institute.

10.1021/jp020895x CCC: $25.00
Published on Web 03/26/2003

The adhesion work is evaluated from the disjoining pressure isotherm at a given subphase composition taking into account the charge regulation for a fatty acid monolayer. The relation of the proposed mechanism to the known experimental facts and observations is discussed.

Formulation of the Problem

The contact angle, which is formed during the substrate withdrawal, plays a crucial role in the LB deposition process. It is well-known that the successful ("dry") deposition is observed at large contact angles ("zipper angle" according to Langmuir[9]), whereas at the zero angle, the entrainment of the water film does not admit the multilayer formation. Large contact angles are necessary for rapid expelling of water from the contact zone. The rate of the water drainage defines the maximum deposition speed of the monolayer.[10] The water drainage is faster, and correspondingly, the maximum deposition speed is larger in the case of the strong adhesion or reactivity between the monolayer and the substrate surface. According to thermodynamic relations, the larger the adhesion work the larger is the contact angle.[11,12] Both the adhesion work and the contact angle depend on the subphase composition near the three-phase contact region. Changes in the local counterion concentrations and in the electric potential distribution, which are expected at dynamic conditions, will result in variations of contact angle, adhesion work and maximum deposition speed. The latter can lead to instability of the film deposition process.

At constant withdrawal velocity, a stationary acute contact angle is usually formed between the floating monolayer and the solid substrate.[12−19] With an increase of the velocity, the dynamic contact angle decreases relative to the static (equilibrium) contact angle. The contact angle varies with the subphase composition, in particular with the subphase pH.[13−18] It is known[20,21] that, in the presence of cadmium chloride with a concentration of $\sim 2.5 \times 10^{-4}$ M, the composition of the floating monolayer changes with increase of the pH from arachidic acid to cadmium arachidate at the pH close to 5.7, i.e., at the same conditions as that given in ref 2. Thus, one can expect that the local pH variations near the three-phase contact line occur during the monolayer deposition, and that they are responsible for both the meniscus oscillations and the composition changes within the deposited monolayer.

The contact angle defines the hydrodynamics within the meniscus region and the maximal velocity of the Langmuir monolayer deposition. The hydrodynamics of the steady movement of the contact line over a solid surface was considered by Huh and Scriven.[22] They analyzed a rather general case of the creeping flow and they considered also the system behavior in the framework of the lubrication approximation. Using the lubrication approximation de Gennes showed that steady state film deposition can be observed, but only if the velocity of the substrate movement is lower than a certain threshold.[23] For small contact angles this threshold is given by the relation

$$V_{max} = \frac{\gamma \theta_e^3}{36\sqrt{3}\eta l} \qquad (1)$$

where $\gamma = \gamma_0 - \Pi$ is the surface tension; γ_0 is the surface tension of the pure solvent; Π is the constant surface pressure under the monolayer deposition; θ_e is the equilibrium contact angle, η is the dynamic viscosity of the liquid; and $l \approx 12$, which is an approximately constant parameter. Hence, the maximum velocity strongly depends on the equilibrium contact angle. If the substrate velocity is larger than V_{max}, the water film entrains between the substrate and the deposited monolayer.[10,23] The maximum of deposition speed is also predicted by a combined molecular-hydrodynamic approach, proposed in refs 24 and 25.

Petrov et al.[10] determined experimentally the maximum deposition rate for monolayers of arachidic acid and cadmium arachidate. The authors obtained relatively high velocity for arachidic acid monolayer deposited at pH 2 (1.3 cm/s) and for cadmium arachidate monolayers deposited at pH 6.8 (0.6 cm/s). For the arachidic acid monolayer at pH = 6.8 in absence of Cd^{2+} ions the maximum deposition rate is very small—much lower than 0.005 cm/s. The authors explained this great difference by difference in reactivities between the monolayer headgroups and the solid surface at different monolayer states varying with the subphase conditions. Note that the withdrawal velocities in ref 2 belong to the range 0.005−0.013 cm/s. Such velocities are smaller than the maximum deposition rate determined in ref 10 in the presence of Cd^{2+} ions and are larger than those observed in the absence of Cd^{2+} ions. Thus, it can be assumed that, under the conditions of ref 2, the maximum deposition rate is not constant and sometimes is lowered below the substrate velocity which is constant during the deposition. Such a decrease of the deposition rate can occur due to the local changes in the subphase composition which give rise to the monolayer transition from the cadmium salt to acid form. If this happens, a stationary deposition regime is not possible and the meniscus becomes unstable.

According to eq 1, the deposition rate decreases with decrease of the contact angle. The contact angle for the withdrawal mode is related to the adhesion work of the hydrophilic heads of the monolayer to the hydrophilic heads of the previously deposited monolayer[12]

$$W = \gamma(1 - \cos \theta_e) \qquad (2)$$

Taking this into account, one can summarize: the monolayer composition, adhesion work, contact angle, and maximum deposition rate are related to each other. Simultaneously, they are defined by the subphase composition. Under dynamic conditions, changes in the local subphase composition (a pH increase and Cd^{2+} concentration decrease) within the meniscus region should be accompanied by change of all this characteristics. A change of the monolayer composition (from cadmium salt to acid form) can lead to a decrease in the adhesion work, resulting in a decrease of the contact angle. The latter leads to a decrease in the maximum deposition rate, which becomes lower than the velocity of the substrate movement, and consequently, leads to meniscus instability. Accordingly, these effects can lead to meniscus oscillations and variation of the composition within the deposited monolayer.

Changes of the monolayer composition, surface energies, and deposition rate were supposed also in refs 4−7 to be responsible for the stripe formation within the deposited lipid (DPPC) monolayers. This changes, however, were related to the substrate induced phase transition from the liquid-expanded to liquid-condensed phase of the monolayer, and therefore, they have another origin than those considered in the present study. The question about the mechanism responsible for the local changes within a fatty acid monolayer during the deposition will be answered next. Note, that the following analysis is specific for systems with dissociating headgroups, such as those considered in ref 2.

Concentration Polarization and Meniscus Oscillations

Considering the LB deposition process one should take into account that a deposited monolayer can contain only the neutral

molecules of fatty acid or of the corresponding salt. At the same time, due to dissociation, the floating monolayer contains negatively charged surface groups. The positive charges (counterions) are located within the diffuse layer what is relatively large (on the order of a debye length of ~100 nm). The charge of monolayer decreases in the three-phase contact region.[8] Passing through this region the monolayer bonds counterions from the subphase, which compensate the surface charge before the transition to the solid substrate. Thus, during the deposition, there should be continuous transport of counterions to the surface. The transport of counterions from distant parts of the diffuse layer requires time. If this transport is not sufficiently fast a deficiency of counterions is produced in vicinity of the three-phase contact line. One usually ignores this circumstance and assumes that deviations from equilibrium are not large.[23] However, in the case of relatively high deposition speeds, the counterion concentrations can substantially decrease relative to their equilibrium distribution, and this decrease should influence the monolayer characteristics in the meniscus region.

Let us consider the flux of negatively charged carboxyl groups that cross the unity length of the three-phase contact line during the monolayer deposition. Partially, the negative charge of the floating monolayer can be already compensated due to the presence of the positively charged 1:1 complex of fatty acid with the divalent metal ions (if they are formed at the surface), as is discussed below. However, there is also a noncompensated part of the negative surface charge which corresponds to the charge of the diffuse layer. The flux transferred by the negatively charged carboxyl groups, which form this noncompensated part of the negative surface charge, is defined by the surface density of these groups and the velocity of the surface movement

$$J_V = (X_{R^-} - X_{RM^+})V \tag{3}$$

where X_{R^-} is the surface density of the dissociated carboxyl groups, X_{RM^+} the surface density of positively charged 1:1 complex of fatty acid with the divalent metal ions, and V the velocity of the surface motion. It is discussed in ref 8 and in the next section that the noncompensated part of the negative surface charge can attain several percents of the total number of the carboxyl groups on the surface (that is, $X_R = 8.3 \times 10^{-6}$ mol/m^2). For the velocity of 0.01 cm/s and 5% of carboxyl groups forming the noncompensated surface charge we find the flux on the unity length of the three-phase contact line

$$J_V = (0.05)(8.3 \times 10^{-6}\,\mathrm{mol/m^2}) \times 10^{-4}\,\mathrm{m/s} \approx 4 \times 10^{-11}\,\mathrm{mol/(m\,s)} \tag{4}$$

The flux of the negative surface charges should be compensated by an equivalent flux of positively charged ions which are located within the diffuse layer in order to fulfill the electroneutrality condition for the deposited monolayer. For a complete compensation, all counterions within the diffuse layers should move with the same velocity as the charged surfaces. The convective flux of the counterions produced by the surface motion is not sufficient to compensate the flux of negative surface charges. The latter takes place since only the parts of the diffuse layers adjacent to the surfaces move with the same velocity as the surfaces in the direction to the contact line. The more distant parts of the diffuse layers move with smaller velocities or even in the opposite direction because of circular structure of the convective flow in the solution, produced by the surfaces (Figure 1). Thus, the monolayer at deposition takes more counterions than is supplied by the convective flux, and therefore a deficit of the counterions is produced near the three-phase contact line.

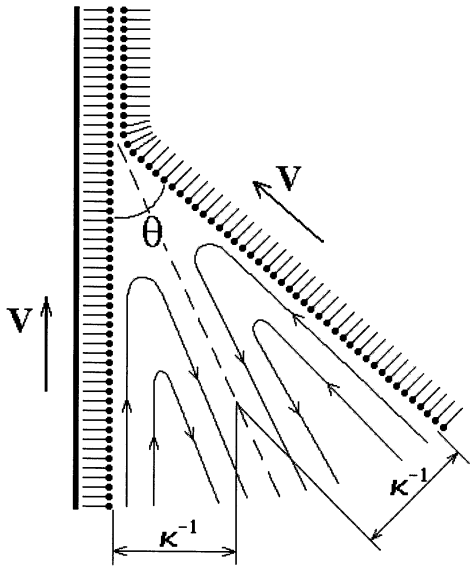

Figure 1. Wedge-like flow in vicinity of the three-phase contact line. V, velocity of the surface motion; θ, microscopic dynamic contact angle; κ^{-1}, thickness of the diffuse layers.

At deposition the monolayer takes practically no coions. At the same time, the convective flux removes more coions from the region near the contact line than it brings to this region, because the coion concentration is larger in the distant parts of the diffuse layers than near the surfaces. As a consequence the coion concentration near the contact line must be also reduced, as compared to the equilibrium conditions. This also corresponds to the electroneutrality condition according to which the counterion concentrations cannot be significantly reduced without the corresponding decrease of the coion concentration. It can be concluded that, in general, the electrolyte concentration near the three-phase contact line decreases at dynamic conditions relative to the equilibrium conditions. Such a process is completely similar to the known process of concentration polarization in dispersions or membrane systems or near electrodes in electrochemical systems.[26−28] Note that the relaxation times of contact angles after stopping the withdrawal motion are usually several times longer than those after dipping and attain above 10 min.[12,13,17] Such large relaxation times after stopping the monolayer deposition can be an evidence of concentration polarization near the three-phase contact line.

The decrease of the electrolyte concentration near the three-phase contact line produces ionic electrochemical potential gradients and the electrodiffusion fluxes of the ions of both signs from the bulk regions to the contact line. The decrease of the ion concentrations and the electrodiffusion fluxes of the ions will be the larger the faster the monolayer transfer. At stationary conditions the electrodiffusion flux of the counterions will be exactly the same as it is necessary to compensate completely for the flux of the negative surface charges, i.e., it will be defined by the difference of the surface flux (eqs 3 and 4) and of the convective flux of the counterions. At the same time, the electrodiffusion flux of the coions will be the same as it is necessary to compensate their convective flux, i.e., to turn their total flux to zero. Thus, under dynamic conditions the stationary balance of individual ions holds due to electrodiffusion fluxes. The deposition process is analogous to "discharging" of cations on a negatively charged surface ("electrode"), i.e.,

the process is similar to a diffusion-limited electrochemical reaction.

In contrast with the equilibrium state, when the electrochemical potentials of ions are equivalent in all points of the solution, under dynamic conditions gradients of the electrochemical potentials are formed, and each point of the solution is characterized by local values of the electrochemical potentials. Though the equilibrium in the system as whole is violated, each separate small volume element of the solution can be approximately considered as one being in local equilibrium. At the same time every such volume element is not in equilibrium with the bulk solution. Nevertheless, for each such volume element an imaginary electroneutral solution can be found that could be in equilibrium with the considered volume element, i.e., that is characterized by the same electrochemical potentials of the ions. The concentrations of acid and salt in this electroneutral solution will be

$$C_{HA} = \sqrt{C'_{A^-} C'_{H^+}}$$

and

$$C_{MA_2} = \sqrt[3]{C'^2_{A^-} C'_{M^{2+}}}$$

where C'_{H^+}, C'_{A^-}, and $C'_{M^{2+}}$ are the local ion concentrations. The decrease of the local concentrations C'_{H^+}, C'_{A^-}, and $C'_{M^{2+}}$ can be characterized by a corresponding decrease of acid and salt concentrations C_{HA} and C_{MA_2} relative to their concentrations in the bulk solution.

Thus, the inner part of the contact region is characterized by smaller quasi-equilibrium acid and salt concentrations than the outer part. Therefore, the meniscus shape deviates from the equilibrium shape. The inner part of the contact region corresponds to an equilibrium contact angle that would exist in the case of reduced acid and salt concentrations in the bulk solution and, therefore, would be smaller than the real equilibrium contact angle, as concluded above. Consequently, the local slope of the meniscus near the contact line and the actual microscopic dynamic contact angle should be smaller. Simultaneously, the region, where the diffuse layers overlap, should increase.

The magnitude of the concentration decrease near the contact line depends not only on the transfer rate but also on the actual microscopic dynamic contact angle. The smaller this angle is, the larger is the distance on which the ions are transferred by the electrodiffusion fluxes. Consequently, to produce the sufficiently large ion fluxes, the concentration difference between the solution near the contact line and the solution out of the diffuse layers must be larger. Due to this dependency a feedback appears in the system: a small initial decrease of the local ion concentrations produces a decrease of the adhesion work of the monolayer (as discussed below) and a decrease of the microscopic dynamic contact angle, which in turn leads to a further decrease of the local ion concentrations. Under certain conditions this mechanism can result in a collapse of the microscopic dynamic contact angle, i.e., when the angle decrease to zero. As a consequence, the maximal deposition rate will decrease below the velocity of the substrate motion, the contact line will move with the substrate, and the water film will entrain between the monolayer and the substrate. Thus, the described mechanism can lead to the meniscus oscillations observed in the experiments. Accordingly the monolayer composition will oscillate too.

The meniscus oscillations can be accompanied by the so-called water-splitting effect which is often observed in electromembrane systems.[29−32] As discussed above, with increasing monolayer transfer velocity the ion concentrations more rapidly decrease near the three-phase contact line, and the corresponding electrodiffusion fluxes increase. However, the electrodiffusion fluxes cannot increase to infinity because they cannot be larger than a limiting diffusion flux, which can be estimated as

$$J_D \approx 2D\kappa^{-1}\frac{C_0}{l} = 2DC_0 \tan\frac{\theta}{2} \quad (5)$$

where J_D is the limiting diffusion flux from the bulk solution (solution out of the diffuse layers) to the contact line per unity length of the contact line, D is the diffusion coefficient, C_0 is the electrolyte concentration in the solution out of the diffuse layers, κ^{-1} is the thickness of the diffuse layer, $l \approx \kappa^{-1}/\tan(\theta/2)$ is the diffusion length that is approximately the distance from the contact line to a place where the diffuse layers begin to overlap, and θ is the microscopic dynamic contact angle (Figure 1). At the very beginning of the process the diffusion length should be determined from the solution of a corresponding nonsteady-state electrodiffusion problem. The diffusion length will increase with time. However, the diffuse layers contain a sufficient number of counterions to compensate the surface charge, so the diffusion length should not increase significantly above the extension of the region, where overlapping of the diffuse layers takes place. For the electrolyte concentration $C_0 = 2.5 \times 10^{-4}$ M and the diffusion coefficient of the order of 10^{-9} m^2/s, this estimation gives

$$J_D \approx 5 \times 10^{-10} \tan\frac{\theta}{2} \text{ mol/(m c)} \quad (6)$$

Though for large contact angles this flux is larger approximately by 1 order of magnitude than that given by eq 4, for small angles this flux can be of the same order or even smaller. Thus for small contact angles the electrodiffusion fluxes of counterions may be not sufficient, to compensate the flux of the negative surface charges.

If the concentration of divalent ions decreases to a critically small value the solution near the contact line becomes comparable to pure water. Because of the deficiency of divalent metal ions, the carboxyl groups begin to join the hydrogen ions at the transition to the substrate surface. In contrast with metal ions, the hydrogen and hydroxyl ions can be generated due to dissociation of water molecules the number of which is practically unlimited. The hydrogen ions are also more mobile than metal ions. Therefore, the monolayer composition should change from salt form to acid form, i.e., from cadmium arachidate to arachidic acid. At the same time, the pH in solution near the contact line should increase because the hydroxyl ions remain in the solution. This process is completely similar to the known process of acid−base generation in ion-exchange membranes that is observed at the conditions of the over-limiting current.[29−32] The adhesion work of fatty acid monolayers strongly decreases in absence of divalent ions at high (neutral or alkaline) pH. At these conditions the maximum deposition rate also strongly decreases.[10] Thus, if the transition of the monolayer composition from the salt form to the acid form occurs (because of the deficiency of divalent metal ions), then the contact line will go up with the substrate practically without monolayer deposition, i.e., the water dissociation facilitates the meniscus instability.

Note, the reaction of water dissociation is relatively slow in the case of pure water. However, the rate of water dissociation increases in the presence of weak acidic (carboxyl and phos-

phate) groups on the surface.[29,30] The rate of water dissociation increases also in the case of a strong electric field that can also happen near the contact line because of the deficiency of counterions. Thus, there are favorable conditions for water dissociation in the meniscus region.

In a regime, when only the hydrogen ions produced by the water dissociation compensate the surface charge within the deposited monolayer, an excess of cadmium ions should remain in the liquid film between the monolayer and the substrate surface. When the number of this ions increases to a certain value, they suppress the concentration polarization. As a result, the monolayer returns to the salt form again. Possibly, the change of the flow pattern after the beginning of instability facilitates this transition. After that, the monolayer transfer becomes faster, the microscopic dynamic contact angle increases, and the meniscus begins to expel water more effectively. The remaining hydroxyl ions recombine with the hydrogen ions in the solution, and the system returns to the initial state.

The considered sequence of the processes can be repeated again and again resulting in the meniscus autooscillations and in the stripes formation within the deposited monolayer.

The Adhesion Work

The described mechanism should agree with the change of adhesion work with concentration. It is well-known that the decrease in the concentration of the counterions (divalent cations and hydrogen ions) in the subphase leads to an increase of the monolayer ionization as well as to the increase of the electrical double-layer thickness. This causes larger double-layer repulsion and a decrease of the adherence of the monolayer to the substrate. Petrov et al.[10] demonstrated that the effect of the double-layer thickness on the maximum deposition rate is small. However, the influence of the monolayer ionization can be much stronger.

If the disjoining pressure is known as a function of the liquid film thickness, the adhesion work can be obtained according to

$$W = \int_{\infty}^{h_0} \Pi(h')\mathrm{d}h' \tag{7}$$

where h_0 is the film thickness corresponding to the deposited monolayer. The molecular, electrical, and other forces acting in the film vary with the film thickness. It is usually assumed in the DLVO theory that the electric potential at interfaces is constant, i.e., it does not vary with the film thickness. This is not correct for the fatty acid monolayers. The superposition of the electrical double layers in the liquid film results in a variation of the counterion concentrations near the interfaces with the film thickness. This leads to a shift of the chemical equilibrium in the reactions of cation association with the carboxyl groups and to a variation of the surface charge density and surface potential with the thickness. Thus, for such monolayers the binding of the counterions should be accounted for to consider the variation of the electrical force with the distance.

The electrostatic component of the disjoining pressure is given by

$$\Pi_{\mathrm{el}} = RT\sum_i C_i(\mathrm{e}^{-z_i F\Psi_0/RT} - 1) \tag{8}$$

where C_i is the concentration of the ith ion in the bulk solution out of the film, z_i is the ion charge, and Ψ_0 is the potential in the symmetry plane if the interfaces are symmetrically charged. We consider the case that the ions presented in the solution are hydrogen ions H^+ with the concentration C_{H^+}, divalent cations, for example Cd^{2+}, with the concentration $C_{M^{2+}}$, and monovalent anions, for example, Cl^-, with the concentration $C_{A^-} = C_{H^+} + 2C_{M^{2+}}$; thus,

$$\Pi_{\mathrm{el}} = RT[C_{H^+}\mathrm{e}^{-F\Psi_0/RT} + C_{M^{2+}}\mathrm{e}^{-2F\Psi_0/RT} + (C_{H^+} + 2C_{M^{2+}})\mathrm{e}^{F\Psi_0/RT} - 2C_{H^+} - 3C_{M^{2+}}] \tag{9}$$

The potential in the symmetry plane Ψ_0 can be obtained from a solution of the Poisson−Boltzmann equation when the surface charge density as a function of the surface potential is known (see Appendix A).

The surface charge is determined by the density and the dissociation degree of fatty acid molecules at the interface and by the number of divalent cations bound to fatty acid. One can write

$$\sigma = -F(X_{R^-} - X_{RM^+}) \tag{10}$$

where X_{R^-} and X_{RM^+} are the surface molar concentrations of the dissociated fatty acid (R^-) and of the 1:1 complex of fatty acid with divalent cations (RM^+), respectively. It is a disputable question whether the positive charged 1:1 complex or the neutral 1:2 complex (R_2M) is formed by the divalent cations with the carboxyl groups in monolayers.[20,21] It is difficult to distinguish from the data on the composition of the deposited LB-films which complex is present in the floating monolayer because both models accounting for either only a 1:1 complex or only a 1:2 complex describe the experimental data equally well.[8,20,21] Therefore, we will consider here all possible models accounting for either only 1:1 complex or only 1:2 complex or both complexes simultaneously.

The dissociation−association processes within the monolayer are described by the reactions

$$RH \rightarrow R^- + H^+ \tag{11}$$

$$R_2M \rightarrow 2R^- + M^{2+} \tag{12}$$

$$R^- + M^{2+} \rightarrow RM^+ \tag{13}$$

for which the equilibrium conditions can be written

$$X_{RH} = K_H X_{R^-} C^S_{H^+} \tag{14}$$

$$X_{R_2M} = K_{M2}(X_{R^-})^2 C^S_{M^{2+}} \tag{15}$$

$$X_{RM^+} = K_{M1} X_{R^-} C^S_{M^{2+}} \tag{16}$$

where X_{RH} and X_{R_2M} are the molar surface concentrations of the nondissociated fatty acid (RH) and of the 1:2 complex of fatty acid with divalent cations (R_2M), respectively; K_H, K_{M1}, and K_{M2} are equilibrium constants; and $C^S_{H^+}$ and $C^S_{M^{2+}}$ are the molar concentrations of H^+ and M^{2+} ions in the solution near the charged surfaces which are dependent on the surface potential Ψ_S according to the Boltzmann equations

$$C^S_{H^+} = C_{H^+}\mathrm{e}^{-F\Psi_S/RT} \tag{17}$$

$$C^S_{M^{2+}} = C_{M^{2+}}\mathrm{e}^{-2F\Psi_S/RT} \tag{18}$$

The total concentration of fatty acid in the monolayer X_R is

given by

$$X_R = X_{R^-} + X_{RH} + 2X_{R_2M} + X_{RM^+} \quad (19)$$

At high surface pressures (about 30 mN/m) the fatty acid monolayer is in a close-packed condensed state, and the surface area per molecule changes only slightly with the surface pressure and pH of the subsolution.[3,33] Therefore, X_R can be approximately considered as a constant.

The monolayer composition is expressed by the surface concentrations of fatty acid X_i in different forms. It varies with the concentrations of the counterions H^+ and M^{2+} near the interface because of the shift of the chemical equilibria. Equations 10 and 14−19 express the so-called charge regulation, i.e., the variation of the surface charge density with the distance between the interfaces and with the bulk concentrations of the counterions. The solution of the Poisson−Boltzmann equation with the additional conditions of eqs 10 and 14−19 allows us to obtain surface charge and potential, potential in the symmetry plane and monolayer composition for the given bulk concentrations and the film thickness. Substituting the potential in the symmetry plane in eq 9 one obtains the electrostatic component of the disjoining pressure. A similar problem was considered in ref 34 but without taking into account the binding of divalent counterions.

The procedure of the determination of the potential at the symmetry plane with accounting for the charge regulation is described in Appendix A. The variation of the surface potential and surface charge density with film thickness and bulk concentrations of the ions was analyzed in ref 8. Neither surface charge nor the surface potential remain constant if the film thickness changes. The surface charge always tends to zero at $h \to 0$. The surface potential increases to infinity at $h \to 0$ for the model that allows only 1:2 complex formation between divalent cations and fatty acid. However if the model of the charge regulation includes the possibility of 1:1 complex formation then the surface potential increases only to a limiting value $-1/2 \ln(K_{M1}C_{M^{2+}})$. This is seen from eq 10 by the substitution of eqs 16 and 18:

$$\sigma = -FX_{R^-}(1 - K_{M1}C_{M^{2+}}e^{-2\tilde{\Psi}_S}) \quad (20)$$

The zero surface charge density corresponds to a zero expression in the bracket when the formation of the 1:1 complex is allowed, and to zero X_{R^-} when the 1:1 complex is absent. The last condition requires an infinitely large surface potential.

Surface charge and surface potential increase with pH and with decrease in the concentration of divalent ions in the solution. The surface charge is negligibly small at small pH. The surface concentration X_{R^-} of the dissociated fatty acid increases with pH but it does not exceed 6% of the total surface coverage X_R. A sharp transition in the monolayer composition is observed in the pH region between 5 and 6. The monolayer is mainly in the nondissociated RH form at small pH and in the form of a complex with the divalent counterions at large pH.

The variation of the electrostatic component of the disjoining pressure and the energy of the electrostatic repulsion are shown in Figures 2 and 3. For the calculations the same parameter values were used as in our previous paper:[8] $X_R = 8.3 \times 10^{-6}$ mol/m^2, $K_H = 6.54 \times 10^4$ dm^3/mol, $K_{M1} = 15.5$ dm^3/mol, and $K_{M2} = 2.5 \times 10^9$ dm^5/mol^2. These parameter values allow the description of the composition of a fatty acid monolayer sufficiently well but these values still have to be defined more precisely because of the reasons discussed in ref 8.

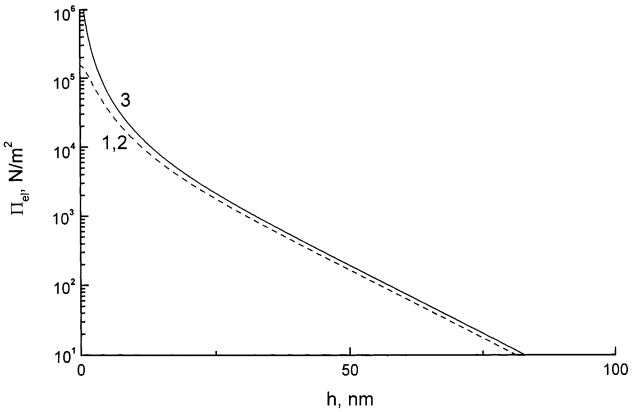

Figure 2. Variation of the electrostatic component of the disjoining pressure with the distance between the charged surfaces for three considered models: (1) formation of 1:1 and 1:2 complexes (K_{M1} = 15.5 dm^3/mol; $K_{M2} = 2.5 \times 10^9$ dm^5/mol^2), (2) formation of only a 1:1 complex (K_{M1} = 15.5 dm^3/mol; $K_{M2} = 0$), (3) formation of only a 1:2 complex ($K_{M1} = 0$; $K_{M2} = 2.5 \times 10^9$ dm^5/mol^2). Other parameters as given in the text.

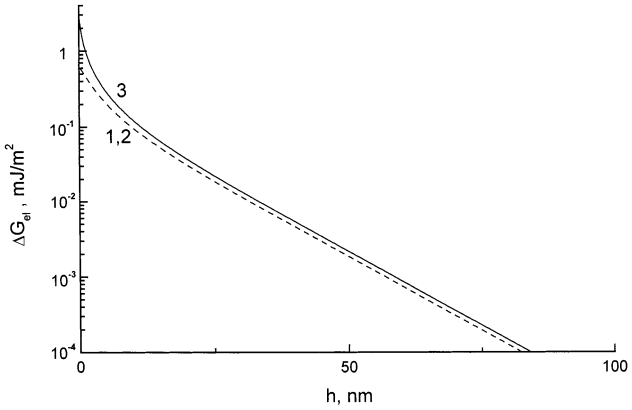

Figure 3. Variation of the electrostatic component of the interaction energy with the distance between the charged surfaces for three considered models: (1) formation of 1:1 and 1:2 complexes (K_{M1} = 15.5 dm^3/mol; $K_{M2} = 2.5 \times 10^9$ dm^5/mol^2), (2) formation of only a 1:1 complex (K_{M1} = 15.5 dm^3/mol; $K_{M2} = 0$), (3) formation of only a 1:2 complex ($K_{M1} = 0$; $K_{M2} = 2.5 \times 10^9$ dm^5/mol^2). Other parameters as given in the text.

The adhesion work can also be obtained in another way, namely, as a difference of the free energies of two surfaces at infinitely large separation and at close contact. This way is proposed in refs 12 and 35. The authors consider the contribution of the double layers to the interaction free energy as

$$\Delta G_{el} = -2\Delta G_{dl} \quad (21)$$

where ΔG_{dl} is the free energy for the formation of a single double layer that they obtained from an equation

$$\Delta G_{dl} = -\int_0^{\Psi_S} \sigma \, d\Psi \quad (22)$$

However, the last equation is correct only in the case of a constant surface potential, and cannot be applied to insoluble monolayers with varying composition. Equation 22 identifies the free energy of a double layer with the double-layer contribution to the surface tension, which is possible to do only at a constant surface potential, as shown by Payens.[36] To be correct one should take into account the change of the chemical part of the free energy. Payens derived a theory with account only for the dissociation of fatty acid, eq 11, in the absence

of divalent counterions. Following Payens, we consider here the case that divalent counterions are present in the solution and can bond to the surface.

The free energy of a monolayer depends on a reference state relative to which it is calculated. The contribution of the double layer to the free energy should be calculated relative to a noncharged state of the monolayer. In the case of absence of divalent counterions, such a state corresponds to the nondissociated state of monolayer, and it is unique.[36] If two or more kinds of counterions can bond to the surface, the noncharged state is not unique because it depends on a relative presence of each counterion in the monolayer. Note, a noncharged state is obtained also when the numbers of positive and negative charges within a monolayer are equivalent (for example, $X_{R^-} = X_{RM^+}$). As we need to know the free energy change during the deposition, we have to find the double-layer contribution for a floating monolayer relative to a noncharged monolayer having the same composition as the deposited monolayer. In fact, we consider an imaginary deposition process having two stages: the first one is a discharging process with obtaining a noncharged monolayer having the same composition as a deposited monolayer, and the second one is the transition of a noncharged monolayer without change the composition to the solid surface. As in the second stage the monolayer is not charged, we can assume that the double-layer contribution belongs only to the first stage.

The composition of deposited and floating monolayers were obtained in our previous paper.[8] They can be characterized by the surface concentrations X^{D}_{RH}, $X^{D}_{R_2M}$, $X^{D}_{R^-}$, and $X^{D}_{RM^+}$ and X^{F}_{RH}, $X^{F}_{R_2M}$, $X^{F}_{R^-}$, and $X^{F}_{RM^+}$, respectively. The surface concentrations X_{RH}, X_{R_2M}, and X_{RM^+} in the floating monolayer are smaller, whereas the concentration X_{R^-} is higher than in the deposited monolayer. Thus, the contribution of the double layer to the change of the free energy is (Appendix B):

$$\Delta G_{dl} = RT\left[X^{D}_{RH}\ln\frac{X^{F}_{RH}}{X^{D}_{RH}} + X^{D}_{R^-}\ln\frac{X^{F}_{R^-}}{X^{D}_{R^-}} + X^{D}_{R_2M}\ln\frac{X^{F}_{R_2M}}{X^{D}_{R_2M}} + X^{D}_{RM^+}\ln\frac{X^{F}_{RM^+}}{X^{D}_{RM^+}} - X^{D}_{R_2M} + X^{F}_{R_2M}\right] - \int_0^{\Psi_S}\sigma\,d\Psi \quad (23)$$

In the absence of divalent ions, the terms corresponding to these ions disappear, the electroneutral state of the monolayer is characterized by $X^{D}_{RH} = X_R$ and $X^{D}_{R^-} = 0$, and one obtains

$$\Delta G_{dl} = RTX_R\ln\frac{X^{F}_{RH}}{X_R} - \int_0^{\Psi_S}\sigma\,d\Psi = RTX_R\ln(1-\alpha) - \int_0^{\Psi_S}\sigma\,d\Psi \quad (24)$$

where α is the degree of dissociation. This equation is an equivalent form to the results obtained in refs 36 and 37.

It is seen that eq 22 does not contain the terms similar to the first terms of eqs 23 and 24, i.e., it neglects the change of the chemical part of the free energy. Equations 23 and 24 provide the correct results which coincide with the free energy change obtained by integration of the disjoining pressure according to eqs 7−9 (while accounting for eq 21) for different concentrations and for different models of surface charge regulation, whereas the use of eq 22 leads to incorrect free energy values unless the surface potential is constant. The direct transition of eq 23 to the case of constant potential is not possible because constant surface potential means constant monolayer composition due to the corresponding equilibrium conditions and, therefore, constant surface charge density. However, the conditions of constant potential and constant surface charge are incompatible, i.e., the condition of a constant potential is not realized in the framework of the considered model. Nevertheless, in some cases the change of surface potential and the corresponding change of monolayer composition during the transfer can be enough small, as shown in our previous paper.[8] In this case the contribution of the first term in eq 23 is small, and the free energy is approximately the same, as given by eq 22.

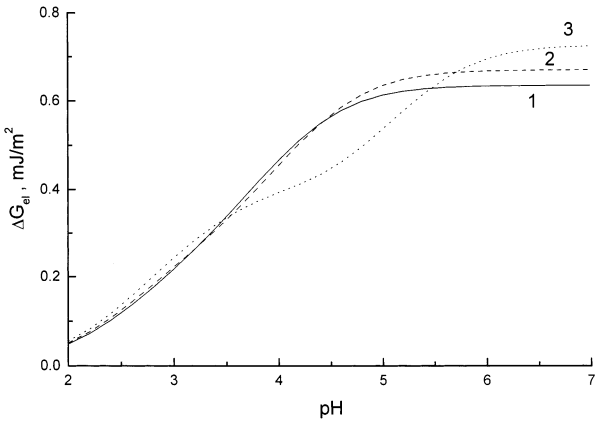

Figure 4. Variation of the double-layer contribution to the free energy of interaction with the pH value and the divalent metal salt concentration in case of formation of 1:1 and 1:2 complexes ($K_{M1} = 15.5$ dm^3/mol; $K_{M2} = 2.5 \times 10^9$ dm^5/mol^2): (1) $C_{M^{2+}} = 2.5 \times 10^{-4}$ M, (2) $C_{M^{2+}} = 1 \times 10^{-4}$ M, (3) $C_{M^{2+}} = 1 \times 10^{-6}$ M. Other parameters as given in the text.

The integral in eq 22−24 for the case of a mixture of uni- and divalent counterions was found in ref 38:

$$\int_0^{\Psi_S}\sigma\,d\Psi = \left[\frac{2(RT)^3\epsilon\epsilon_0 C_{M^{2+}}}{F^2}\right]^{1/2}\{(e^{-\tilde{\Psi}_S}+2)\sqrt{(r+2)e^{+\tilde{\Psi}_S}+1} - 3\sqrt{r+3} + r[\coth^{-1}\sqrt{(r+2)e^{+\tilde{\Psi}_S}+1} - \coth^{-1}\sqrt{r+3}]\} \quad (25)$$

where $r = C_{H^+}/C_{M^{2+}}$ and $\tilde{\Psi}_S = F\Psi_S/RT$. In the case of a 1:1 electrolyte this integral transforms to a well-known result[12,35]

$$\int_0^{\Psi_S}\sigma\,d\Psi = 4\left[\frac{2(RT)^3\epsilon\epsilon_0 C_{H^+}}{F^2}\right]^{1/2}\left(\cosh\frac{\tilde{\Psi}_S}{2} - 1\right) \quad (26)$$

To integrate the disjoining pressure according to eqs 7−9, we have to choose the minimal film thickness h_0. This point requires comments. As we consider pointlike ions we naturally have to substitute $h_0 = 0$. It is known, however, that for distances smaller than 10 Å the Poisson−Boltzmann equation describes the electrostatic interactions not favorably (sufficiently) good. By using eq 23 we make the same error because in order to calculate the composition of the deposited monolayer we also use the Poisson−Boltzmann equation. We can, however, hope that the contribution of small distances to the total integral of the disjoining pressure (and to the total monolayer composition change) is relatively small, i.e., the discussed error is small.

The contribution of the double layer to the free energy of interaction for the three considered models are shown in Figures 4−6. In all cases the energy of the electrostatic repulsion increases with pH. For the models accounting for the 1:1 complex of Cd^{2+} ions with carboxyl groups, the energy for the electrostatic repulsion increases with the concentration of metal

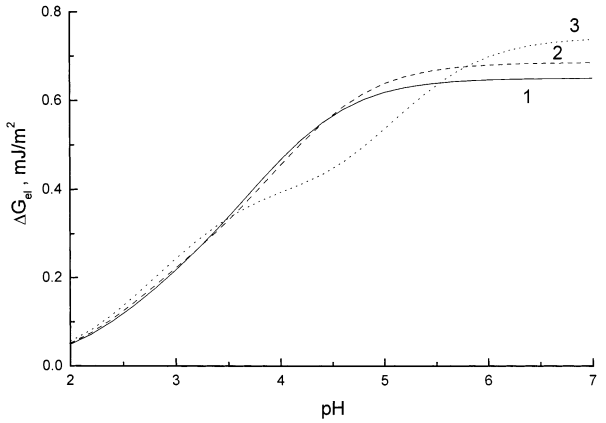

Figure 5. Variation of the double-layer contribution to the free energy of interaction with the pH value and the divalent metal salt concentration in case of only 1:1 complex formation ($K_{M1} = 15.5$ dm^3/mol; $K_{M2} = 0$): (1) $C_{M^{2+}} = 2.5 \times 10^{-4}$ M, (2) $C_{M^{2+}} = 1 \times 10^{-4}$ M, (3) $C_{M^{2+}} = 1 \times 10^{-6}$ M. Other parameters as given in the text.

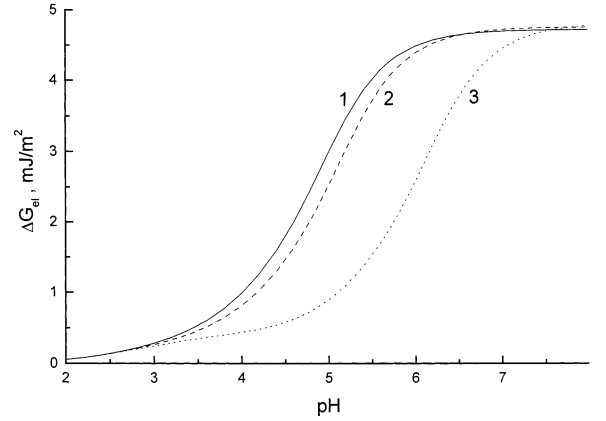

Figure 6. Variation of the double-layer contribution to the free energy of interaction with the pH value and the divalent metal salt concentration in case of only 1:2 complex formation ($K_{M1} = 0$; $K_{M2} = 2.5 \times 10^9$ dm^5/mol^2): (1) $C_{M^{2+}} = 2.5 \times 10^{-4}$ M, (2) $C_{M^{2+}} = 1 \times 10^{-4}$ M, (3) $C_{M^{2+}} = 1 \times 10^{-6}$ M. Other parameters as given in the text.

ions at pH above 5.7. In the case of only 1:2 complex formation, the energy for the electrostatic repulsion increases with the concentration of metal ions only at pH above 7, and it is much larger than in the presence of 1:1 complexes.

The van der Waals component of the free energy of the interaction of two monolayers was evaluated in refs 12 and 35 by using several models. All estimations show that the contribution of van der Waals forces to the free energy of interaction is very small, 1−2 orders of magnitude smaller than the double-layer contribution, and smaller than the experimental values of the free energy of interaction. The same models can be applied also in our case, and we obtain the contribution of van der Waals forces to be approximately on the same order of magnitude because the thickness of the water core between the contacting monolayers differs not very significantly. The sum of the double-layer contribution and of the van der Waals forces contribution is positive and cannot explain the strong adhesion of the deposited monolayers requiring large negative values of the free energy of interaction. A similar effect is observed also for the measured forces between charged bilayers in the presence of divalent counterions which are often significantly more attractive than expected from the DLVO theory.[39] To explain the contradiction we have to assume that a strong attractive component is neglected in the analysis.

Several hypothesis are discussed in refs 12 and 35 which can explain the nature of the neglected attractive component. The effect is often attributed to attractive ion-correlation forces.[39] It might be also related to hydrogen bonds or electrostatic attraction between the discrete periodic distributions of opposite charges.[12] The quantitative verification of this hypothesis for the considered system is a matter of further investigations. Here this question remains open.

Nevertheless, for the aims of the present study, we actually need the relative change of the interaction energy with pH and the divalent ion concentration rather than its absolute value. It is interesting to see that for the systems considered in refs 12 and 35 the relative change of the double-layer contribution corresponds surprisingly good with the relative change of the measured free energy of interaction. This is possible when other contributions are only weakly dependent on the ion concentrations. Hopefully, this is applicable also to the system considered here. If it so, we can expect that the total free energy of interaction changes with pH and the divalent ion concentration in a similar way as the double-layer contribution.

Thus, as we have seen (Figures 4−6) the double-layer repulsion increases with increase of the pH above the equilibrium pH 5.7 and decrease of the cadmium salt concentration below the equilibrium $C_{M^{2+}} = 2.5 \times 10^{-4}$ M (the last holds for pH above 5.7 or 7 depending on the model), and it is quite expectable that this leads to a corresponding decrease of the total attraction energy, i.e., to a decrease of the adhesion work, and consequently, to a decrease of the contact angle according to the eq 2. However, we cannot here quantitatively estimate this effect, because the absolute values of the work of adhesion are unknown, and we have to be restricted only to a qualitative analysis.

Nevertheless, the supposition about the contact angle decrease with decrease of the counterion concentrations is supported by some experimental data on the deposition of fatty acid monolayers in the pH interval 4−7 in the presence and absence of divalent cations.[14,15] As a consequence of the contact angle decrease, the maximum rate of the monolayer transfer also decreases with decrease of the divalent cations concentration and pH increase. This follows from eq 1 and is also in agreement with the experimental data.[10,40] A similar correlation of the monolayer ionization, contact angle, and maximum monolayer transfer rate is also observed for long-chain alkylamines in the presence of divalent counterions (cf. the results of refs 10 and 12). Thus, the proposed mechanism correlates with the experimental data and is supported by the analysis of the free energy of interaction.

Conclusions

The proposed mechanism of the meniscus oscillations and the stripes formation is based on the supposition of concentration polarization near the contact line at the monolayer deposition. Concentration polarization is a phenomenon accompanying always the motion of a charged surface relative the bulk solution. For the case of monolayer deposition, the estimation of this effect shows that its magnitude can be sufficient to produce a significant local change of the subphase composition. The presence of this effect is indicated by the very slow relaxation of contact angles after stopping the withdrawal motion. The proposed mechanism corresponds to the observed meniscus behavior during oscillations and agrees with numerous experimental data on adhesion work, contact angles, and maximum monolayer deposition rate. It is also obvious that the meniscus oscillations can be accompanied by a water-splitting effect often observed in cases of strong concentration polarization.

The results of the theoretical analysis indicate that concentration polarization always accompanies deposition processes of charged monolayers. However, usually concentration polarization does not lead to dramatic changes of the monolayer composition. Only stationary deviations of dynamic characteristics from their static values are mostly observed. However, in the special case considered here, the arachidic acid monolayer at pH = 5.7 is in a state very close to its transition from the cadmium salt to the acid form, and a relative small pH variation can initiate this transition leading to significant fast changes of adhesion, dynamic contact angle, and maximum deposition rate.

The performed analysis of the concentration polarization is based on a simplified consideration which neglects the real meniscus shape and the exact solution of the convective diffusion problem but the main tendencies of the system behavior will be maintained by an exact consideration.

Further studies of meniscus oscillations should be focused on rigorous investigations of the static and dynamic contact angles at different subphase compositions. These studies should be accompanied by simultaneous measurements of the maximum deposition rate, disjoining pressure, and adhesion work.

Acknowledgment. Financial assistance by the Bundesministerium für Bildung, Wissenschaft, Forschung und Technologie (BMBF) and Ukrainian Ministry of Education and Science (common project UKR-014-98) is gratefully acknowledged.

Appendix A

For the present case the Poisson−Boltzmann equation takes a form

$$\frac{d^2\Psi}{dy^2} = -\frac{F}{\epsilon_0\epsilon}[C_{H^+}e^{-F\Psi/RT} + 2C_{M^{2+}}e^{-2F\Psi/RT} - (C_{H^+} + 2C_{M^{2+}})e^{F\Psi/RT}] \quad \text{(A1)}$$

with the boundary condition for the normal component of the electric field at the interfaces

$$\left(\frac{\partial\Psi}{\partial y}\right)_S = -\frac{\sigma}{\epsilon_0\epsilon} \quad \text{(A2)}$$

and the condition of the zero electric field in the symmetry plane

$$\left(\frac{\partial\Psi}{\partial y}\right)_0 = 0 \quad \text{(A3)}$$

where Ψ is the electric potential, ϵ the dielectric constant, ϵ_0 the permittivity of vacuum, and σ the surface charge density: the last is supposed to be approximately equivalent at the solid−liquid and air−liquid interfaces.

The solution of the Poisson−Boltzmann equation for a liquid film having the thickness h in the presence of monovalent and divalent counterions is[8,34]

$$\tilde{\Psi}_S = \tilde{\Psi}_0 + \ln\left\{(1-u_2)sn^2\left[K(k) - \frac{\kappa' h\sqrt{u_1-u_2}}{4}\exp\frac{\tilde{\Psi}_0}{2}, k\right] + u_2\right\} \quad \text{(A4)}$$

$$\sigma = -\{2\epsilon_0\epsilon RT[C_{H^+}(e^{-\tilde{\Psi}_S} - e^{-\tilde{\Psi}_0}) + C_{M^{2+}}(e^{-2\tilde{\Psi}_S} - e^{-2\tilde{\Psi}_0}) + (C_{H^+} + 2C_{M^{2+}})(e^{\tilde{\Psi}_S} - e^{\tilde{\Psi}_0})]\}^{1/2} \quad \text{(A5)}$$

where $\tilde{\Psi}_S = F\Psi_S/RT$, $\tilde{\Psi}_0 = F\Psi_0/RT$, $\kappa'^2 = 2F^2(C_{H^+} + 2C_{M^{2+}})/\epsilon_0\epsilon RT$; $sn(t,k)$ is the elliptic function with the modulus $k = \sqrt{(1-u_2)/(u_1-u_2)}$; $K(k) = \int_0^1 dt/[(1-t^2)(1-k^2t^2)]^{1/2}$ is the quarter period of the elliptic function, and

$$u_{1,2} = \frac{C_{H0} + C_{M0} \pm \sqrt{(C_{H0} + C_{M0})^2 + 4C_{A0}C_{M0}}}{2C_{A0}} \quad (u_1 \geq 1, u_2 \leq 0) \quad \text{(A6)}$$

are the functions of the ion concentrations at the symmetry plane $C_{H0} = C_{H^+}\exp(-\tilde{\Psi}_0)$, $C_{M0} = C_{M^{2+}}\exp(-2\tilde{\Psi}_0)$, and $C_{A0} = (C_{H^+} + 2C_{M^{2+}})\exp(\tilde{\Psi}_0)$.

By using the equilibrium conditions (eqs 14−16 and 17−18), eqs 10 and 19 can be written in the form

$$X_R = X_{R^-}(1 + K_H C_{H^+}e^{-\tilde{\Psi}_S} + K_{M1}C_{M^{2+}}e^{-2\tilde{\Psi}_S} + 2K_{M2}X_{R^-}C_{M^{2+}}e^{-2\tilde{\Psi}_S}) \quad \text{(A7)}$$

$$\sigma = -FX_{R^-}(1 - K_{M1}C_{M^{2+}}e^{-2\tilde{\Psi}_S}) \quad \text{(A8)}$$

The surface concentration X_{R^-} can be expressed from eq A8 and substituted into eq A7, producing

$$X_R = -\frac{\sigma}{F(1 - K_{M1}C_{M^{2+}}e^{-2\tilde{\Psi}_S})}\left(1 + K_H C_{H^+}e^{-\tilde{\Psi}_S} + K_{M1}C_{M^{2+}}e^{-2\tilde{\Psi}_S} - \sigma\frac{2K_{M2}C_{M^{2+}}e^{-2\tilde{\Psi}_S}}{F(1 - K_{M1}C_{M^{2+}}e^{-2\tilde{\Psi}_S})}\right) \quad \text{(A9)}$$

This equation gives the surface charge density as a function of surface potential for known ion concentrations in the solution. The set of eqs A4, A5, and A9 allows us to find surface charge density, surface potential, and potential at the symmetry plane. These equations include as parameters the film thickness, the bulk concentrations of the ions, the surface coverage X_R, and the equilibrium constants. Consequently, σ, Ψ_S, and Ψ_0 will be functions of these parameters. The set of eqs A4, A5, and A9 was solved numerically. The solution can be obtained in the following way. For a chosen value Ψ_0 one can find the surface charge and surface potential from eqs A5 and A9. Then substituting Ψ_S and Ψ_0, one can find the film thickness h that corresponds to this solution.

Appendix B

The transition from a noncharged to a charged floating monolayer can be also divided in three stages: (1) the fatty acid molecules dissociate according to the reaction of eq 11, (2) the neutral complexes R_2M dissociate according to the reaction of eq 12, (3) the excess of the dissociated molecules R^- and positive complexes RM^+ recombine according to the reaction

$$R^- + RM^+ \rightarrow R_2M \quad \text{(B1)}$$

that is a combination of the reactions of eqs 12 and 13. Each of the processes is characterized by the free energy change

$$\Delta\bar{G}_k = \sum_i \mu_i^k - \sum_j \mu_j^k \quad \text{(B2)}$$

which is given by a difference of the sum of chemical potentials of the initial components μ_i^k and the sum of chemical potentials of the products μ_j^k in each process (the chemical potentials are taken at the surface). In the first process the surface

concentrations X_{R_2M} and X_{RM^+} does not change, and therefore, the contribution of this process to the free energy change is

$$\Delta G_1 = \int_{X_{R^-}^D}^{X_{R^-}^D + \Delta X_{RH}} \left(RT \ln K_H + RT \ln \frac{C_{H^+}^S X_{R^-}}{X_{RH}} \right) dX_{R^-} = \int_0^{\sigma^*} \Psi_S \, d\sigma + RT \ln(K_H C_{H^+}) \Delta X_{RH} + RT[(X_{R^-}^D + \Delta X_{RH}) \ln (X_{R^-}^D + \Delta X_{RH}) - X_{R^-}^D \ln(X_{R^-}^D) + (X_{RH}^D - \Delta X_{RH}) \ln(X_{RH}^D - \Delta X_{RH}) - X_{RH}^D \ln(X_{RH}^D)] \quad \text{(B3)}$$

where $\sigma^* = -F\Delta X_{RH}$ and ΔX_{RH} is the change of the surface concentration X_{RH} at the transition from the deposited to floating monolayer (all ΔX_i are defined here as positive, i.e., as absolute values).

In the second process the surface concentrations X_{RH} and $X_{RM}{}^+$ are constant and therefore is

$$\Delta G_2 = \int_{X_{R^-}^D + \Delta X_{RH}}^{X_{R^-}^D + \Delta X_{R^-} + \Delta X_{RM^+}} \left(RT \ln(K_{M2}) + RT \ln \frac{C_{M^{2+}}^S X_{R^-}^2}{X_{R_2M}} \right)$$

$$\frac{dX_{R^-}}{2} = \int_{\sigma^*}^{\sigma} \Psi_S \, d\sigma + RT \ln(2K_{M2} C_{M^{2+}}) \frac{\Delta X^*}{2} + RT \Big[(X_{R^-}^D + \Delta X_{R^-} + \Delta X_{RM^+}) \ln(X_{R^-}^D + \Delta X_{R^-} + \Delta X_{RM^+}) - (X_{R^-}^D + \Delta X_{RH}) \ln(X_{R^-}^D + \Delta X_{RH}) - \frac{\Delta X^*}{2} + \frac{1}{2}(2X_{R_2M}^D - \Delta X^*) \ln(2X_{R_2M}^D - \Delta X^*) - X_{R_2M}^D \ln(2X_{R_2M}^D) \Big] \quad \text{(B4)}$$

where $\sigma = -F(\Delta X_{R^-} + \Delta X_{RM^+})$, $\Delta X^* = \Delta X_{R^-} + \Delta X_{RM^+} - \Delta X_{RH} = 2(\Delta X_{R_2M} + \Delta X_{RM^+})$, and ΔX_i are the changes of the corresponding surface concentrations at the transition from the deposited to floating monolayer (absolute values).

For the third process we find in a similar way (X_{RH} is constant)

$$\Delta G_3 = \int_{X_{R_2M}^F \Delta - X_{RM^+}}^{X_{R_2M}^F} \left(RT \ln \frac{K_{M1}}{K_{M2}} + RT \ln \frac{X_{R_2M}}{X_{RM^+} X_{R^-}} \right) dX_{R_2M} = RT \Big[\ln \frac{K_{M1}}{K_{M2}} \Delta X_{RM^+} + X_{R_2M}^F \ln(X_{R_2M}^F) - (X_{R_2M}^F - \Delta X_{RM^+}) \ln (X_{R_2M}^F - \Delta X_{RM^+}) + \Delta X_{RM^+} + X_{RM^+}^F \ln(X_{RM^+}^F) - X_{RM^+}^D \ln (X_{RM^+}^D) + X_{R^-}^F \ln(X_{R^-}^F) - (X_{R^-}^F + \Delta X_{RM^+}) \ln(X_{R^-}^F + \Delta X_{RM^+}) \Big] \quad \text{(B5)}$$

Note, eqs B3 and B4 include both chemical and electrical contributions considered separately by Payens.[36] Following Payens we assume that the rearrangement of the counterions (and coions) within the diffuse layer does not produce a contribution to the free energy change because these ions have the same electrochemical potential as the ions in the bulk solution as the equilibrium between the diffuse layer and the bulk is always established.

Combining eqs B3 and B5 and using the equilibrium conditions for a floating monolayer eqs 14−16 one obtains with eq 23 the contribution of the double layer to the free energy change.

References and Notes

(1) Roberts, G. G., Ed. *Langmuir−Blodgett Films*; Roberts, G. G., Ed.; Plenum Press: New York, 1990.
(2) Mahnke, J.; Vollhardt, D.; Stöckelhuber, K. W.; Meine K.; Schulze, H. J. *Langmuir* **1999**, *15*, 8220.
(3) Kurnaz, M. L.; Schwartz, D. K. *J. Phys. Chem.* **1996**, *100*, 11113.
(4) Spratte, K.; Chi, L. F.; Riegler, H. *Europhys. Lett.* **1994**, *25*, 211.
(5) Spratte, K.; Riegler, H. *Langmuir* **1994**, *10*, 3161.
(6) Riegler, H.; Graf, K. *Colloids Surf. A* **1998**, *131*, 215.
(7) Riegler, H.; Spratte, K. *Thin Solid Films* **1992**, *210/211*, 9.
(8) Kovalchuk, V. I.; Zholkovskij, E. K.; Bondarenko, N. P.; Vollhardt, D. *J. Phys. Chem.* **2001**, *105*, 9254.
(9) Langmuir, I. *Science* **1938**, *87*, 493.
(10) Petrov, J. G.; Kuhn, H.; Möbius, D. *J. Colloid Interface Sci.* **1980**, *73*, 66.
(11) Clint, J. H.; Walker, T. *J. Colloid Interface Sci.* **1974**, *47*, 172.
(12) Petrov, J. G.; Angelova, A. *Langmuir* **1992**, *8*, 3109.
(13) Gaines, G. L., Jr. *J. Colloid Interface Sci.* **1977**, *59*, 438.
(14) Neuman, R. D. *J. Colloid Interface Sci.* **1978**, *63*, 106.
(15) Neuman, R. D.; Swanson, J. W. *J. Colloid Interface Sci.* **1980**, *74*, 244.
(16) Buhaenko, M. R.; Richardson, R. M. *Thin Solid Films* **1988**, *159*, 231.
(17) Aveyard, R.; Binks, B. P.; Fletcher, P. D. I.; Ye, X. *Colloids Surf. A* **1995**, *94*, 279.
(18) Aveyard, R.; Binks, B. P.; Fletcher, P. D. I.; Ye, X. *Thin Solid Films* **1992**, *210/211*, 36.
(19) Peng, J. B.; Abraham, B. M.; Dutta, P.; Ketterson, J. B. *Thin Solid Films* **1985**, *134*, 187.
(20) Bloch, J. M.; Yun, W. *Phys. Rev. A* **1990**, *41*, 844.
(21) Ahn, D. J.; Franses, E. I. *J. Chem. Phys.* **1991**, *95*, 8486.
(22) Huh, C.; Scriven, L. E. *J. Colloid Interface Sci.* **1971**, *35*, 85.
(23) De Gennes, P. G. *Colloid Polym. Sci*. **1986**, *264*, 463.
(24) Petrov, J. G.; Petrov, G. P. *Langmuir* **1998**, *14*, 2490.
(25) Petrov, G. P. *J. Chem. Soc., Faraday Trans.* **1997**, *93*, 295.
(26) Dukhin, S. S. *Conductivity and Electrokinetic Properties of Dispersion Systems*; Naukova Dumka: Kiev, 1975 (in Russian).
(27) Lakshminarayanaiah, N. *Transport Phenomena in Membranes*; Academic Press: New York, 1969.
(28) Levich, V. G. *Physicochemical Hydrodynamics*; Prentice Hall, Englewood Cliffs, NY, 1962.
(29) Simons, R. *Electrochim. Acta* **1984**, *29*, 151; *Electrochim. Acta* **1986**, *31*, 1175.
(30) Zabolotskii, V. I.; Shel'deshov, N. V.; Gnusin, N. P. *Uspekhi Khimii* **1988**, *57*, 1403 (in Russian).
(31) Zholkovskij, E. K.; Kovalchuk, V. I. *Elektokhimiya* **1988**, *24*, 74 (in Russian).
(32) Ramirez, P.; Manzanares, J. A.; Mafe, S. *Ber. Bunsen-Ges. Phys. Chem.* **1991**, *95*, 499.
(33) Johann, R.; Vollhardt, D. *Mater. Sci. Eng. C* **1999**, *8*−*9*, 35.
(34) Ninham, B. W.; Parsegian, V. A. *J. Theor. Biology* **1971**, *31*, 405.
(35) de Feijter, J. A.; Vrij, A. *J. Colloid Int. Sci.* **1979**, *70*, 456.
(36) Payens, Th. A. J. *Philips Res. Rep.* **1955**, *10*, 425.
(37) Helm, C.; Laxhuber, L.; Lösche, M.; Möhwald, H. *Colloid Polym. Sci.* **1986**, *264*, 46.
(38) DeSimone, J. A. *J. Colloid Int. Sci.* **1978**, *67*, 381.
(39) Israelachvili, J. N. *Intermolecular and Surface Forces*; Academic Press: London, 1997.
(40) Veale, G.; Peterson, I. R. *J. Colloid Interface Sci.* **1985**, *103*, 178.